

# The influence of spin-forbidden monomer excitations on spin-allowed electron transfer and electron-localized states of mixed-valence and single-valence dimeric systems

J.R. Reimers<sup>a</sup>, N.S. Hush<sup>a,b</sup>

<sup>a</sup> *Department of Physical and Theoretical Chemistry, University of Sydney, Sydney, NSW 2006, Australia*

<sup>b</sup> *Department of Biochemistry, University of Sydney, Sydney, NSW 2006, Australia*

Received 15 June 1994

## Abstract

Models for the spin-allowed absorption spectra of weakly interacting dimeric systems are usually cast in terms of perturbed localized spin-allowed excitations on each chromophore, enhanced by the addition of electron-transfer excitations between them. We show that locally spin-forbidden processes on individual chromophores, when coupled weakly to either unpaired spins or other spin-forbidden processes on other chromophores, become spin-allowed and may perturb spectra and excited state photochemistry. In neutral dimers, some doubly excited states are quite low lying, and it is possible for one of these to constitute the lowest lying spin-allowed excited state. In dimer radical ions, a (possibly quite intense) band is generally expected to lie very close to the triplet absorption energy of each isolated monomer. Particular examples are considered, as well as a model system consisting of an ethylene dimer in a stacked configuration typical of that found in large  $\pi$ -systems such as the primary electron donor in the photosynthetic reaction centre, stacked phthalocyanines, acene dimers, stretched norbornadiene-type systems, etc. The results apply more generally than this, however, being relevant to all weakly interacting molecular or inorganic systems.

*Keywords:* Spin-forbidden excitation; Spin-allowed electron transfer; Electron-localized states; Mixed-valence systems; Single-valence systems

## 1. Introduction

In order to understand the function of photo-induced charge-transfer systems, it is almost always necessary to model, with reasonable accuracy, the electronic absorption and/or emission spectra of the isolated or combined donor and acceptor chromophores; typically, calculations for more than one valence state of the system are also required. Usually, this is accomplished by determining the ground state of the system using Hartree–Fock self-consistent-field (SCF) methodology, followed by a limited configuration-interaction (CI) calculation involving states produced by spin-allowed single excitations from the ground state. Such an approach often provides a very good description of the spectra of the individual chromophores, and facilitates discussion of the spectra of the combined donor and acceptor in terms of minor changes to the intra-chromophore states combined with new inter-chromophore charge-transfer states. The neglect of higher excitations is justified primarily on energy grounds: double and

higher excitations are typically of very much higher energy than the single excitations of interest and are hence assumed to perturb them insignificantly. While this result is applicable to most isolated molecules, it has significant shortcomings for all single-valent closed-shell weakly interacting chromophore pairs. This is because spin-forbidden excitations on each chromophore can interact with each other, in a similar fashion to the spin-allowed excitations, but with the result that new spin-allowed and spin-forbidden states arise. As the energy of, say, a monomer triplet state can be considerably less than that of the corresponding singlet, these new states appearing in weakly interacting complexes can be of low energy, possibly even being the lowest energy spin-allowed state.

The consequences of this have not been fully explored in the context of electron-transfer phenomena, long-range information communication and molecular-electronic device design. They are, however, well-known in other areas. Consider, for example, the interaction through space of neutral naphthalene molecules. The

prediction of low-energy singlet excited states formed by the interaction of two naphthalene-monomer triplet states was first made by Murrell and Tanaka [1]. Evidence for their existence comes from dynamics studies in naphthalene crystals highly populated by molecules in their lowest triplet state (triplet excitons): formation of singlet-coupled naphthalene pairs provides a long-lived component to the fluorescence spectrum. Schematically, the origin of this state for a closed-shell dimer is shown in Fig. 1 as excited state 1, where the highest occupied molecular orbital (HOMO) and lowest unoccupied molecular orbital (LUMO) for two (different) monomers, named A and B, are shown. The arrows indicate that this state arises from two counteracting electron-transfer transitions from the ground state, one transferring an electron of spin  $\beta$  from A to B while the other transfers an electron of spin  $\alpha$  from B to A. An alternative representation of this transition, apparent from an inspection of the resulting electron configuration, is to view it as two spin-forbidden triplet absorptions occurring on each isolated chromophore. This view allows the energy of this transition, at infinite separation, to be determined immediately as simply the sum  $\nu = {}^3A + {}^3B$  of the triplet absorption energies of each monomer unit,  ${}^3A$  and  ${}^3B$ .

The spin-forbidden manifolds of monomers also contribute to the spin-allowed states of weakly interacting open-shell systems, e.g. mixed-valence systems. A familiar example of this occurs when radical or triplet character is imparted by one molecule onto a second nearby closed-shell molecule. It permits, for example, the intensification [2] of direct triplet absorptions of a chromophore in the presence of  $O_2$ . The simpler, related process by which a radical B can induce triplet absorptions in a closed-shell chromophore A is indicated schematically in Fig. 2 excited state 3, where the HOMO and LUMO orbitals of A and B are shown. There, the arrows indicate that this state can be conceived as arising from a double electron-transfer excitation be-

tween non-spin-adapted configurations, taking a  $\beta$  electron from the HOMO of A to the (half-occupied) HOMO of B and an  $\alpha$  electron from the HOMO of B to the LUMO of A. A similar result is obtained by considering this transition as the combination of a spin-forbidden triplet absorption on A and a spin-forbidden spin flip on B; this view allows the energy of the transition at infinite separation to be identified as simply the triplet absorption energy of chromophore A,  ${}^3A$ . An example of this process is the intensification of phthalocyanine  $\pi \rightarrow \pi^*$  triplet transitions in Cu phthalocyanine as a result of the unpaired spin of the  $Cu^{2+}$  ion [3].

All weakly interacting chromophores will have low-energy states with an origin similar to those described above; in this paper, we investigate the characteristic behaviour of these and other similar states as the coupling increases, and consider possible effects that they could have on photochemical electron-transfer processes. Initially, we introduce a model which is in some sense characteristic of all electron-transfer systems, and applies specifically for an important class of systems: the through-space interaction of two stacked ethylene molecules. Generally, the introduction of through-bond coupling, geometric distortions or metal atoms does not change the types of effects to be seen; specifically, this model applies directly to important situations such as the bacteriochlorophyll dimer  $BChl_2$  which forms the primary electron donor in the photosynthetic reaction centre [4,5], stacked phthalocyanines [6–8], crown ether complexes [9], stacked aromatics (e.g. [10]), norbornadiene-based systems, etc., which have overlapping  $\pi$  clouds. Finally, we apply this model in illustrative examples to the ethylene dimer and its cation,  $BChl_2^+$ , and the inorganic charge-transfer system pentammine pyridyl ruthenium(III). The geometries used for the model and for these examples are shown in Fig. 3.

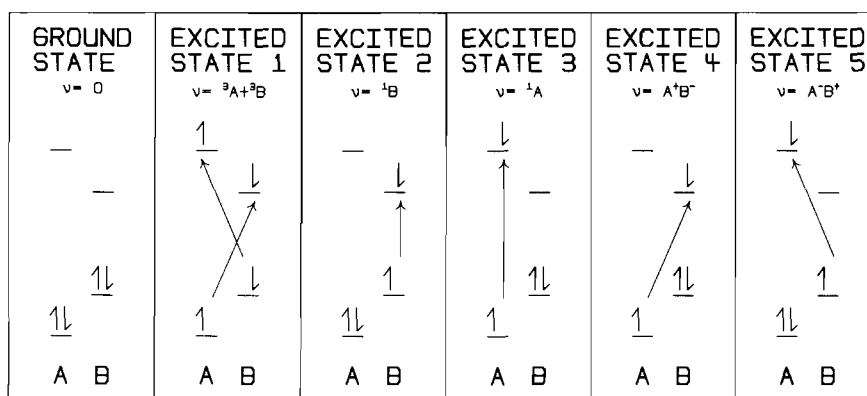


Fig. 1. Single determinants (non-spin-adapted configurations) describing the ground state and low lying spin-allowed excited states of a closed-shell AB complex at infinite separation. Relative energies are indicated by  $\nu$ , see text. The arrows describe single-electron excitations from the ground-state determinant which produce each excited state determinant.

GROUND STATE $\nu = 0$	EXCITED STATE 1 $\nu = {}^1\text{HT}$	EXCITED STATE 2 $\nu = \text{HT}+{}^3\text{B}$	EXCITED STATE 3 $\nu = {}^3\text{A}$	EXCITED STATE 4 $\nu = {}^1\text{B}^+$	EXCITED STATE 5 $\nu = \text{HT}+{}^1\text{A}^+$	EXCITED STATE 6 $\nu = \text{HT}+{}^1\text{B}$	EXCITED STATE 7 $\nu = {}^1\text{A}$
— — ↑ ↓↑	— — ↑↓ ↑	— ↑ ↑ ↓	↑ — ↓ ↑	— ↑ — ↓↑	↑ — — ↑↓	— ↓ ↑ ↑	↓ — ↑ ↑
A B	A B	A B	A B	A B	A B	A B	A B

Fig. 2. Single determinants (non-spin-adapted configurations) describing the ground state and low lying spin-allowed excited states of a closed-shell molecule A and an infinitely separated open-shell molecule B. Relative energies are indicated by  $\nu$ , see text. The arrows describe single-electron excitations from the ground-state determinant which produce each excited state determinant.

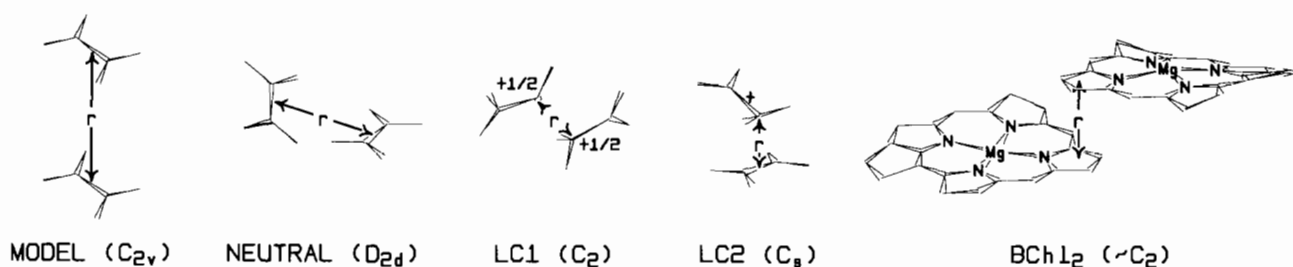


Fig. 3. Geometry of the model system ( $D_{2h}$  symmetry is reduced to  $C_{2v}$  by stretching one of the CC bonds), the neutral ethylene dimer [11] and possible structures LC1 and LC2 for its cation [12], and BChl<sub>2</sub>, the special pair of the photosynthetic reaction centre [5].

## 2. Basic model

### 2.1. Description

The geometry used in the basic model is shown in Fig. 3 and contains two ethylene molecules stacked one directly on top of the other, a system of  $D_{2h}$  symmetry that is, except where noted, relaxed to  $C_{2v}$  by stretching one of the CC bonds slightly (see later). We consider the basic qualitative features of the spectra of neutral or ionic clusters of this type, varying only one geometric variable, the interplanar separation  $r$ , from an essentially infinite separation of 6 Å through the region 4.5 to 3.5 Å in which significant intermolecular interactions occur, down to 2 Å where strong intermolecular interactions lead to the development of new chemical bonds and, in this case, the formation of cyclobutane. In many ways, effects seen in real systems such as extending the  $\pi$  system over many atoms (e.g. from ethylene to benzene to porphyrin or pentacene), geometry changes, and the appearance of through-bond coupling mechanisms serve only to change the length scale of  $r$ , the energy scale, symmetry-related effects such as the location of avoided crossings at small  $r$ , or even the quantitative accuracy of the molecular energy operator used (especially at small  $r$ ); they preserve the basic qualitative features of interest.

It is now possible to evaluate properties of electron-transfer systems using ab initio techniques, especially those relating to the interaction of different systems each in their ground electronic state [13]. Excited state properties are much more difficult to obtain, however; methods are just being developed for studying the monomers of single-ring  $\pi$  systems [14,15] and small polyenes [16]. Herein, we use the CNDO/S-CI method [17,18] for organic molecules and the related INDO/S-CI method [19,20] for metal-containing molecules. Their advantages include ready applicability to large systems, including most systems of electron-transfer interest, e.g. the photosynthetic reaction centre [21], and their quantitative success in describing the properties of a large range of chromophores. In this application, their major deficiency is that they are not parameterized for intermolecular interactions; while they are known to provide excellent qualitative and quantitative performance through the region of medium to weak interaction (say 3–4 Å), poor quantitative performance may result in the strong interaction region. As these are model calculations, poor quantitative performance is not necessarily a problem; it is, however, important to recognize that CNDO and INDO do display the correct qualitative features during the compression and dissociation of molecular complexes: they use Slater-type atomic orbitals whose overlap shows the correct

qualitative feature of exponential decay at large separation, unlike Gaussian orbitals (in practical calculations, e.g. with Gaussian orbitals [22], large basis sets containing diffuse functions are required in order to obtain a qualitatively correct description over a desired range of  $r$ ). The advantage of correct qualitative behaviour at short ( $< 3 \text{ \AA}$ ) and long ( $> 5 \text{ \AA}$ )  $r$  is that the results obtained in the intermediary region, the key region of interest, will also be qualitatively correct and hence descriptive of general physical phenomena.

An important aspect of the calculation of the properties of dimeric ions is the choice made as to whether the Fock operator is to treat the charge as localized on one monomer or delocalized over both. In principle, if a sufficiently large configuration interaction (CI) calculation is performed, then the final results are independent of this choice, but it is rarely possible to accomplish this. If the distances are short and the interactions strong, then a delocalized description is undoubtedly the best. For weak coupling, a localized or mixed-valence description (i.e. one in terms of a monomer with one particular electronic charge interacting weakly with a monomer of a different electronic charge) provides the best description of the ground state of the system. However, in this situation, single-determinant wavefunctions, obtained by rearranging the electrons within localized molecular orbitals, provide very poor descriptions of the charge-transfer excited states [23,24]. Consider the lowest energy charge-transfer process which transfers a single charge from, say, an ionic to a neutral monomer; this is achieved simply by changing the orbital assignment of one electron. Regarding all other valence electrons as a 'frozen core' allows the process to be viewed as one which produces an ion with the core of the neutral and a neutral molecule with the core of the ion. This is not a particularly good description of the excited state, and has with it a 'reorganization energy' associated with the relaxation of the frozen core. For the symmetric  $D_{2h}$  model geometry at infinite separation  $r$ , CNDO/S without any CI calculates this energy to be  $11\,000 \text{ cm}^{-1}$  whereas it should be zero. The effects of core relaxation may be included through the use of full electron correlation (i.e. including all possible excitations from the core), but this is impractical: inclusion of all states singly excited from both determinants lowers the energy to  $5700 \text{ cm}^{-1}$ , while including all such single and double excitations in a Møller–Plesset 2nd order perturbation theory calculation (MP2) lowers the energy to just  $1400 \text{ cm}^{-1}$ .

Conceptually, the best way to treat this problem is to determine molecular orbitals for the two cases in which the charge is located on either monomer independently. The charge-transfer excitation energies can then be determined using the method of corresponding orbitals [25,26] to construct the interactions

between the required non-orthogonal electronic configuration states. This method is usually only applied to calculate the energy of the first excited state of dimeric ions, and becomes very expensive for higher states as the number of different electronic configurations involved may increase rapidly.

We use a method which separates the molecular orbitals into two spaces – an active set, in which all of the orbitals and interactions pertinent to the problem being considered are included, and a second inactive core. For the ethylene dimer outside the strong interaction region, we select the four  $\pi$  orbitals as the active set, and keep the  $\sigma$  orbitals inactive. In an MCSCF calculation, the two electronic configurations corresponding to the charge localized on each monomer are given equal weight, and so the core orbitals adjust to describe a system with an equally partitioned charge: in one sense they are an average of the core orbitals that would be obtained for isolated neutral and ionic molecules. A CI calculation is then performed in which all possible excitations amongst the small active space are included, as well as all single excitations from each of these states involving orbitals from the inactive space; this allows the charge to localize or delocalize according to the strengths of the interactions involved, and results in a good description of the electronic states of the system. Semi-empirical schemes like CNDO/S, which are parameterized to reproduce spectra at the single-excitation CI level, can give poor results if additional correlation is also included; this scheme minimizes such problems as the extra correlation included treats all important states equivalently. As a result, all transitions amongst the active space are well represented, including charge-transfer transitions. The MCSCF calculation can be performed using spin-restricted open-shell Hartree–Fock (ROHF) techniques [27], and requires little more computational resources than does a standard CNDO/S calculation on a neutral molecule. It gives good results when the core does not interact significantly with the active orbitals; this is an assumption which is implicitly made in conventional applications of CNDO/S, and is believed to be generally appropriate. This method also has the advantage that the electronic spin is restricted to physically meaningful values at all stages of the calculation, and rigorously avoids the spin-contamination problems that make unrestricted Hartree–Fock (UHF) calculations unreliable.

In our model, the four  $\pi$  orbitals are orientated parallel, but those on different monomers overlap in a  $\sigma$  fashion, so this complex does not have strict  $\sigma$ – $\pi$  separability. For medium to weak interactions (say  $r > 3.5 \text{ \AA}$ ), the properties of the four  $\pi$  orbitals are not significantly affected by the presence or absence of the  $\sigma$  orbitals. Hence, to simplify our model, we proceed by eliminating the  $\sigma$ -type basis functions (i.e. the entire inactive space) from the CNDO/S calculation, and the

CNDO/S Hamiltonian thus reduces to the Pariser–Parr–Pople (PPP) Hamiltonian [28,29], allowing analytical solution to various aspects of the problem. Note that the all-valence basis set is used for the applications described in Section 3; however, in these, expanded active spaces are included in order to treat the strongly interacting region reliably.

If the symmetry of our model ethylene dimer is constrained to be  $D_{2h}$ , then no electronic state has a non-zero dipole moment. This applies even for states of an electron-transfer nature, as the energy of the electron transfer from one ring to the other will be degenerate with the energy of the reverse process, and any trivial interaction between these two transitions will serve to delocalize the excitation. Such a situation is somewhat unrealistic, as even molecular zero-point motion serves to produce nuclear geometries which instantaneously break symmetry. To allow for this, we carry out all calculations at a  $C_{2v}$  geometry obtained by slightly extending one of the two CC bond lengths by 0.05 Å, the zero-point displacement of a C=C bond stretch motion. This facilitates localization of excitations and charges at large monomer separations; charge-transfer bands can then readily be identified since, at large separation, they produce excited states whose dipole moments  $\mu$  differ from that of the ground state by  $er$ , and we define the fraction of an electron transferred between monomers during an electronic excitation as

$$x = \frac{|\Delta\mu|}{er} \quad (1)$$

The charge localization which we describe as a function of a molecular vibration is in itself actually quite an interesting phenomenon. Displacing the mode in the reverse direction reverses the direction of the vibrationally induced dipole moment, and hence these vibrations have large dipole-moment derivatives and hence very intense IR transitions. An example of this is the coupling between opposite pyrrole groups *within* a single  $\pi$  porphyrin cation [30]; there, the appearance of a new intense IR band is a characteristic signature of the production of a  $\pi$ -cation radical during porphyrin oxidation [31].

## 2.2. Single-valence systems: the neutral model ethylene dimer

Results obtained for the five lowest excited states of the neutral model ethylene dimer are shown in Fig. 4, and descriptions of the asymptotic electron assignments of these states are given in Fig. 1. At large separation  $r$ , all the oscillator strength is associated with states 2 and 3: these correspond to localized  ${}^1\pi \rightarrow \pi^*$  transitions on the individual monomers A and B, and have no charge transfer quality so that  $x=0$ . Their

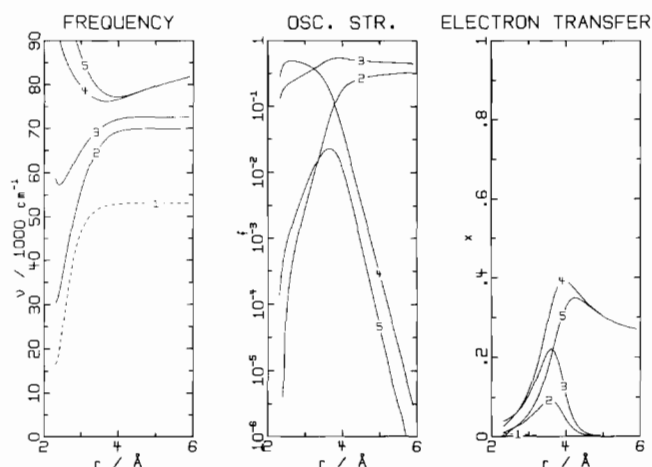


Fig. 4. The frequency  $\nu$ , oscillator strength  $f$  and fraction  $x$  of an electron transferred during spin-allowed  $\pi$  electronic transitions in the neutral model ethylene dimer. The ground state has  $A_1$  symmetry in the  $C_{2v}$  point group; excited states are: —  $B_2$  and ---  $A_1$  symmetry. The excited states are described in Fig. 1; briefly, 1 is the 'double-triplet' state, 2 and 3 are localized  $\pi \rightarrow \pi^*$  states, and 4 and 5 are charge-transfer  $\pi \rightarrow \pi^*$  states.

asymptotic energies are  ${}^1B=69\,900$  and  ${}^1A=72\,600$   $\text{cm}^{-1}$ , where monomer B is taken to have the stretched CC bond in the asymmetric  $C_{2v}$  model structure.

Charge-transfer transitions, states 4 and 5 in Fig. 4 and Fig. 1, are also predicted, each of which transfers an electron from the HOMO of one monomer to the LUMO of the other. The energies of these transitions are predicted at large separation to be:

$$\begin{aligned} \Delta E(A^-B^+) &= E_{\text{LUMO}}^A - E_{\text{HOMO}}^B - \frac{1}{r} \\ \Delta E(A^+B^-) &= E_{\text{LUMO}}^B - E_{\text{HOMO}}^A - \frac{1}{r} \end{aligned} \quad (2)$$

As, in a PPP-type calculation, the effect of increasing the CC bond length in an ethylene molecule is to raise the HOMO orbital by the same amount as the LUMO is lowered, these two expressions evaluate to give the same quantity at large  $r$ , and hence the two transitions become degenerate. The fraction of an electron transferred, as designated as  $x$ , increases steadily as the separation increases to  $r=4$  Å, but remains constant beyond this as our geometric perturbation has failed to lift the degeneracy of the two transitions. They have very little oscillator strength at large separation, but with decreasing distance this increases exponentially until about  $r=4$  Å, the region of onset of significant intermolecular interaction.

The lowest-energy transition, 1, shown in Fig. 1 and Fig. 4 is the 'double-triplet' excitation; its energy, calculated to be  $53\,000$   $\text{cm}^{-1}$ , is simply the sum  $\nu = {}^3A + {}^3B$  of the triplet absorption energies of each monomer ( ${}^3B=24\,800$  and  ${}^3A=28\,200$   $\text{cm}^{-1}$ ). As this state involves no *net* charge transfer, the transition energy is inde-

pendent of distance for separations larger than 3.5 Å; at shorter distances, the magnetic attraction of the two spinning subsystems lowers the transition energy. If, as in our model, the dimer point group is non-degenerate, then state 1 is totally symmetric; it interacts strongly with the ground state at short distances, and an avoided crossing of the potential surfaces occurs at  $r=2.3$  Å.

The 'double-triplet' band arises as a double excitation from two different doubly occupied orbitals to two different unoccupied orbitals. In terms of spin-adapted electronic configurations, this excitation has associated with it two singlet electronic states and one triplet. The singlet states are usually referred to as being either 'singlet coupled' or 'triplet coupled'; the lower energy band is the triplet coupled band, and asymptotically reduces to the non-spin-adapted configuration shown as band 1 in Fig. 1, while the energy of the singlet coupled band is found, at infinite separation, to be the sum of the energies of the monomeric singlet  $\pi \rightarrow \pi^*$  bands, i.e.  ${}^1A + {}^1B = 142\,500$   $\text{cm}^{-1}$ , and is not shown in the figures. Both bands are allowed in two-photon absorption spectroscopy; at separations of  $r=3.5$  Å typical of the interplanar separation in dimeric  $\pi$  complexes, the individual one-photon oscillator strengths shown in Fig. 4 are large, and hence these two-photon bands could be quite intense. Our calculations show that almost all the two-photon intensity goes into the high-frequency singlet-coupled excitation, and that the low-frequency triplet-coupled band has very little intensity.

### 2.3. Mixed-valence systems: the model ethylene dimer cation

Results for the seven lowest bands obtained for the model ethylene dimer cation are shown in Fig. 5, and their asymptotic description in terms of non-spin-adapted configurations is shown in Fig. 2. At large separation, the ground state has the charge (or charge hole) localized on monomer B; the bands numbered 1, 2, 5 and 6 have  $x=1$  and are of a charge-transfer nature, carrying it to monomer A. At these separations, only band 7, the  $\pi \rightarrow \pi^*$  band localized on the neutral monomer at energy  ${}^1A = 72\,500$   $\text{cm}^{-1}$ , and band 4, the  $\pi \rightarrow \pi^*$  band localized on the ionic monomer at energy  ${}^1B^+ = 41\,700$   $\text{cm}^{-1}$ , have significant oscillator strength.

Band 1 is the ground-state hole-transfer (HT) band which, at infinite separation, simply interchanges the identity of the neutral and ionic molecules. In Fig. 5 its asymptotic energy does not approach zero due to the different CC bond lengths used for the monomers: this results in the introduction of a small reorganizational energy of  $\text{HT} = 1600$   $\text{cm}^{-1}$ . At separations shorter than 4 Å, the sharp decrease in the fraction of an electron transferred indicates that the hole becomes delocalized over both monomer units. In practical calculations, the

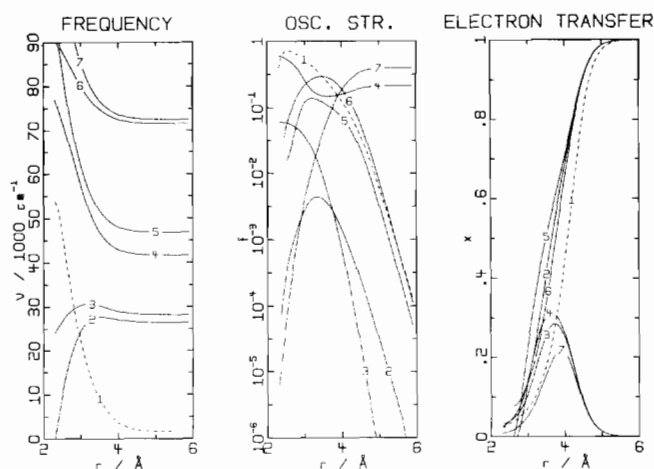


Fig. 5. The frequency  $\nu$ , oscillator strength  $f$  and fraction  $x$  of an electron transferred during spin-allowed  $\pi$  electronic transitions in the model ethylene dimer cation. The ground state has  $A_1$  symmetry in the  $C_{2v}$  point group; excited states are: —  $B_2$  and ---  $A_1$  symmetry. The excited states are described in Fig. 2; briefly, 1 is the hole-transfer state, 2 and 3 are 'local triplet' states, 4 and 5 derive from  $\pi \rightarrow \pi^*$  excitations on a charged monomer, and 6 and 7 derive from  $\pi \rightarrow \pi^*$  excitations on a neutral monomer.

precise value of  $r$  at which this changeover occurs will depend on any reorganization energies (both internal and environment-related) associated with geometric changes between a neutral and an ionic monomer. At small  $r < 3$  Å in the strong interaction region, the energy of this band increases extremely rapidly (the slope is  $-6$  eV/Å at 2.6 Å), and as a result quantitative performance may be impaired in practical calculations.

Bands 5 and 6 are the excitations obtained by following the hole-transfer excitation of band 1 with the localized  $\pi \rightarrow \pi^*$  excitations of bands 4 and 7. Band 6 is of lower energy than band 7 despite the additional  $1600$   $\text{cm}^{-1}$  required for the HT excitation as the  $\pi \rightarrow \pi^*$  absorption of a neutral ethylene molecule at the extended bond length is  ${}^1B = 69\,900$   $\text{cm}^{-1}$ , considerably less than that at the observed bond length (band 7),  ${}^1A = 72\,500$   $\text{cm}^{-1}$ . Band 5 is somewhat higher energy than band 4 as in this case the two effects reinforce rather than compete: the absorption energy of an ion at the geometry of monomer A is  ${}^1A^+ = 45\,200$   $\text{cm}^{-1}$ , greater than that of band 4,  ${}^1B^+ = 41\,700$   $\text{cm}^{-1}$ .

Two relatively low-energy, spin-allowed bands, labelled 2 and 3 in Fig. 2 and Fig. 5, appear in the spectrum of the cation, and arise from the spin-forbidden manifolds of the monomers. Band 3 occurs at the triplet absorption frequency of monomer A,  ${}^3A = 28\,200$   $\text{cm}^{-1}$ . Band 2 occurs at  $26\,400$   $\text{cm}^{-1}$ , the triplet absorption frequency of monomer B,  ${}^3B = 24\,800$   $\text{cm}^{-1}$ , plus the HT energy of  $1600$   $\text{cm}^{-1}$ . Both bands gain intensity in the region of significant interaction, and they could be observed in the optical absorption spectrum of dimeric cations, lying between the (usually IR-frequency) hole transfer band, band 1 and the usual  $\pi \rightarrow \pi^*$  bands. In

systems with more than one occupied  $\pi$  orbital per monomer, local transitions from the SHOMO to the HOMO on the ion could also be expected to lie in this region, however, and could be considerably more intense. At short distances, state 2 falls lower in energy than the ground state: if a dimer cation forms with an equilibrium separation in this range, then, as state 2 is of different symmetry to the ground state, the reaction will be symmetry forbidden. This is a well-known result [32], and so this model is seen to describe qualitatively correctly the asymptotic behaviour at small separations  $r$ .

The electronic states depicted in Fig. 2 are in terms of non-spin adapted configurations, as is appropriate asymptotically at large  $r$ . State 3 appears as a double excitation in this representation. In actual calculations, spin-adapted linear combinations of single-determinant wavefunctions are used. Determinants 3 and 7 (amongst others) are not eigenfunctions of spin and are self-interacting; spin adaptation of the single-excitation state 7 requires the generation of state 3, and hence this state is implicitly included in a singles-excitation CI calculation. Indeed, the problem of two  $\alpha$  and one  $\beta$  electron in three half-occupied orbitals produces three spin-adapted states, two of them doublets and one a quartet; the two doublets reduce to states 3 and 7 asymptotically. State 5 is, however, a legitimate double-excitation: a standard singles-excitation CI calculation would not include states like this, and may miss important features of photoinduced electron transfer.

Additional computational problems arise when the two chromophores are symmetrically related. If the molecular orbitals are constrained to conform to the nuclear symmetry, then the orbitals will be delocalized over both monomers. At large separation, this enforced delocalization mixes the closed and open shells and as a result the ground state and single-determinant excited states are poorly represented. Inclusion of single-excitation CI is insufficient to provide quantitatively reliable excitation energies, and all possible excitations amongst the  $\pi$  space should be included in the calculation. The results obtained by the computational scheme used here vary continuously as the  $C_{2v}$  distortion is relaxed.

Note that high-order excited states obtained by combining excitations 2 or 3 with 4 or 5 occur at around  $70\,000\text{ cm}^{-1}$  and are not shown in Fig. 5 for clarity.

### 3. Predictions for specific systems

#### 3.1. The ethylene dimer

The actual neutral ethylene dimer is weakly bound and has [11] the  $D_{2d}$  structure shown in Fig. 3 with a bond-centre separation of  $r=3.8\text{ \AA}$ . The energies of

its singlet excited states are shown in Fig. 6 as a function of the bond-centre separation, evaluated using CNDO/S including all possible excitations amongst the four  $\pi$  orbitals as well as all possible single excitations from each of these states. Owing to the large number of states thus generated, a scheme is implemented which includes specifically the 200 lowest energy states  $i$  but includes the effects of all other states  $k$  using the MP2 perturbation theory. This expresses the effective matrix element  $H_{i,i'}$  in terms of its direct component  $H_{i,i'}^0$  and a 'through-bridge'-like term expressed, following Larsson [33], as

$$H_{i,i'} = H_{i,i'}^0 + \sum_k \frac{H_{i,k}H_{i',k}}{(E_i + E_{i'})/2 - E_k} \quad (3)$$

where  $E_j$  is given as the sum of the molecular orbital energies of each electron in the (spin-adapted) determinant  $j$ . Note that, in order to avoid very large perturbations due to small energy denominators, this calculation is actually performed for only a small subset of 20 or so relevant, low-energy excitations amongst subset  $i$ .

The results are qualitatively similar to those found earlier for the model dimer, the major difference being that the double-triplet excitation, band 1, is not totally symmetric in this degenerate point group and hence it can cross the ground state at very short distances. The relative energies are significantly different, however, now reflecting accurately those of ethylene: inclusion of the  $\sigma$  excitations lowers the ethylene monomer

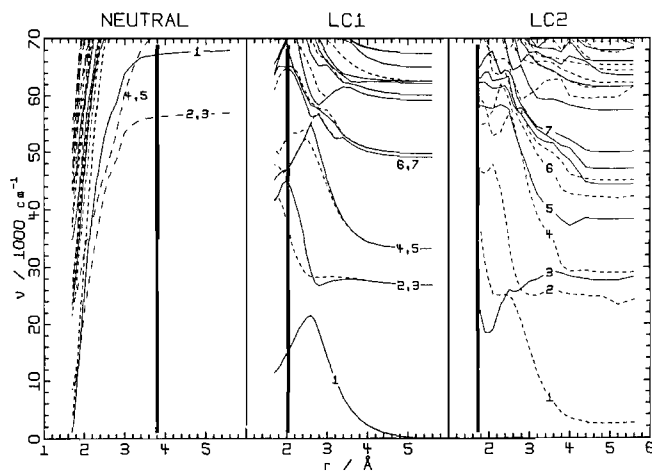


Fig. 6. The frequency of spin-allowed excitations in the neutral ethylene dimer [11], and that for two postulated [12] structures LC1 and LC2 for its cation as a function of the inter-ethylene separation  $r$  as defined in Fig. 3; the vertical bars indicate the actual value of  $r$  for each complex. State symmetries are: for the neutral-point group is  $D_{2d}$ , ground state is  $A_1$ , excited states —  $A_1$ , - - - E, and - - - other; for LC1-point group is  $C_{2v}$ , ground state is B, excited states — A and - - - B; for LC2-point group is  $C_{2v}$ , ground state is  $A'$ , excited states —  $A''$  and - - -  $A'$ . The state numbering for the neutral molecule is described in Fig. 1, while that for the cations LC1 and LC2 is described in Fig. 2.



transitions (bands 2 and 3) from 72 500 to 55 500  $\text{cm}^{-1}$ , close to its observed value [34] of  $\sim 55\,000\ \text{cm}^{-1}$ ; similarly the ethylene monomer triplet absorption frequency is increased from 23 100 to 33 800  $\text{cm}^{-1}$ , close to its observed [2] value of  $\sim 35\,000\ \text{cm}^{-1}$  so that the predicted infinite-separation double-triplet absorption energy (band 1) increases to 67 600  $\text{cm}^{-1}$ , unfortunately well above the  $\pi \rightarrow \pi^*$  absorption. The double-triplet band is thus likely to be difficult to observe in the ethylene dimer itself.

Two possible structures, named LC1 and LC2, have been suggested [12] for the metastable ethylene dimer cation, and these are shown in Fig. 3; LC1 is found to be energetically preferred [12]. Other structures, including one with  $D_{2h}$  symmetry were located [12] as saddle points very close in energy to these, and it is possible that more detailed calculations may modify the ordering. All have short intermolecular separations, and constitute strongly interacting chromophores with electronic structures qualitatively different from those found at large separations. The doublet-state energies calculated as for the neutral dimer are also shown in Fig. 6; here, the active space is chosen to be the four  $\pi$  orbitals and two  $\sigma^*$  orbitals which strongly interact at short distances. Structure LC1 has the charge delocalized while structure LC2 has it localized on one ethylene group and hence has a finite reorganization energy at infinite separation. Qualitatively, the results are similar to those found for the model, with symmetry differences giving rise to different patterns of avoided crossings. Experimentally, it should be possible to discriminate between these two possible structures based on their electronic absorption spectrum: LC1 is predicted to absorb strongly in the red at 18 000  $\text{cm}^{-1}$  with an oscillator strength of  $f=0.23$ , while LC2 has only weak absorptions at much higher energy. For the  $D_{2h}$  structure of Jungwirth and Bally (corresponding to our model geometry at  $r=2.65\ \text{\AA}$ ), CNDO/S predicts an intense absorption at 35 000  $\text{cm}^{-1}$ ; inclusion of  $\sigma$  functions does not significantly affect the  $\pi$ -only results for this band, shown in Fig. 5. Note, however, that all these structures are located in the strong interaction region, and hence the results obtained using CNDO may not be quantitatively reliable.

### 3.2. Photosynthetic reaction centre cation

The 'special pair' BChl<sub>2</sub> forms the photosynthetic reaction centre *Rhodospseudomonas viridis* consisting [4,5] of two nearly-parallel pseudo-planar bacteriochlorophyll (BChl) molecules which interact via just one of the pyrrole rings on each chromophore, see Fig. 3. The two planes are separated by 3.5  $\text{\AA}$ , the intermagnesium spacing is 7.5  $\text{\AA}$ , and the key chromophore elements have approximate  $C_2$  symmetry.

For the BChl<sub>2</sub> cation, INDO/S calculations predict spin-allowed electronic absorptions below those of the Q bands at 1700 (band 1 from Fig. 2, medium), 4000 (band 2, medium), 6000 (band 3, weak), and 9000 (SHOMO  $\rightarrow$  HOMO, very weak)  $\text{cm}^{-1}$ . Band 1 is well represented, being found experimentally [35,36] at 2750  $\text{cm}^{-1}$ ; no bands at 4000 and 6000  $\text{cm}^{-1}$  are observed, however, but a medium intensity band at 8000  $\text{cm}^{-1}$  and several weak shoulders at  $\sim 9000$  and 10 500  $\text{cm}^{-1}$  are observed [35,37,38]. The 8000  $\text{cm}^{-1}$  band has been assigned [36] as the SHOMO  $\rightarrow$  HOMO transition, despite its considerable intensity and the fact that this transition is forbidden in unsubstituted porphyrins and bacteriochlorins. CNDO and INDO, when used with Mataga-Nishimoto integrals as is necessary to reproduce singlet spectra, usually underestimate triplet absorption frequencies, however, and similar calculations for the triplet states of the isolated halves of the reaction centre's special pair predict 4000 and 6000  $\text{cm}^{-1}$ , the same frequencies as predicted for doublet transitions in the dimer cation. Actually, the triplet states of BChl have been observed [39] at 8200  $\text{cm}^{-1}$ ; hence it is probable that the intense absorption seen in the dimer cation actually corresponds to the process of band 2 and not to the previously postulated SHOMO  $\rightarrow$  HOMO transition. This is pursued elsewhere [19].

### 3.3. $\text{Ru}^{3+}(\text{NH}_3)_5\text{-pyridine}$

This complex forms a simple electron-transfer system in which the two chromophores are considered to be the weakly coupled pyridine  $\pi$  system and ruthenium 4d orbitals. In its ground state in aqueous solution, this complex has an unpaired electron placed in the ruthenium 'd <sub>$\pi$</sub> ' orbital, a d orbital of t<sub>2g</sub> symmetry that points at and interacts with the nitrogen p <sub>$\pi$</sub>  orbital. INDO/S calculations predict that three electronic excitations should have significant intensity: the ligand  $^1\pi \rightarrow \pi^*$  band (band 4, Fig. 2) at  $\nu=35\,000\ \text{cm}^{-1}$ ,  $f=0.33$ ; the ligand  $^3\pi \rightarrow \pi^*$  band (band 3) at  $\nu=28\,000\ \text{cm}^{-1}$ ,  $f=0.014$ , and what is largely a ligand  $\rightarrow$  metal charge-transfer band (band 1) at  $\nu=24\,000\ \text{cm}^{-1}$ ,  $f=0.034$ . Experimentally, two or three unresolved [40] bands are seen in the spectrum [41] of this complex centred at  $\nu=38\,000\ \text{cm}^{-1}$  (strong, known to be band 4) and 32 000 and 35 000  $\text{cm}^{-1}$  (weak shoulders, unassigned). The accuracy of INDO/S for ligand  $\rightarrow$  metal charge-transfer transitions is not yet established, and such a state is also likely to experience a significant blue solvent shift [42]. For pyridine itself the triplet state is calculated by INDO/S to lie at 26 000  $\text{cm}^{-1}$ , and is found experimentally at 32 000  $\text{cm}^{-1}$  [43,44] with approximately the same band width as is inferred [40] for the  $\text{Ru}^{3+}(\text{NH}_3)_5\text{-pyridine}$  shoulder. We thus assign the observed weak shoulder at 32 000  $\text{cm}^{-1}$  to the intensified ligand triplet absorption band, band 3, sug-



gesting that the charge-transfer band may constitute the higher energy shoulder.

#### 4. Conclusions

Discussion of the spectroscopy of weakly interacting dimeric systems usually involves consideration of the interaction of the spin-allowed excitations on each chromophore, and the single-electron-transfer processes between them. We see that interactions between spin-forbidden processes on each chromophore give rise to low-energy spin-allowed processes in dimeric complexes. Sometimes, these cause double excitations to produce either the lowest-energy spin-allowed excited state, or one quite close to it. In closed-shell systems, the triplet absorption energy usually exceeds half the singlet absorption energy; molecules for which the triplet/singlet ratio falls below 1/2, making the double-triplet excitation the lowest spin-allowed excitation, do occur, however, e.g. for long linear acenes like tetracene and pentacene, for which the lowest triplet/singlet frequency ratios are observed [45] to be 0.484 and 0.462, respectively. Indeed, the acenes are interesting as they tend naturally to dimerize [10]. Interesting effects, especially on fluorescence spectra, are likely to occur when acenes are used in bridged electron-transfer applications.

For electron-transfer systems involving one closed-shell and one open-shell chromophore, significant effects are likely to occur when the monomer triplet bands are lower in energy than the excitations between the open shell and the other orbitals on its monomer. Then, new bands may appear in absorption spectra, and significant perturbations to fluorescence spectra, especially that following charge-transfer, may occur. Also, the possibility of long-distance information communication is possible as the intensification or other effects induced by the presence of an open-shell chromophore may be transferred along a molecular bridge to some distant site.

The coupled spin-forbidden monomer bands, although they can often be thought of as essentially double excitations in nature, appear to have characteristic very low two-photon absorption intensities, making detection by this method difficult.

The determination of the excited states of weakly interacting systems poses significant problems for any computational technique; we have shown how it is possible to use simple techniques like CNDO/S and INDO/S to obtain results which are qualitatively descriptive over a wide geometry range from dissociation through the region of primary interest, that of weak coupling, and into the strong interaction region. Our method stresses the importance of equally correlating all states of interest, remembering that these methods are parameterized to give good results with restricted

configuration interaction, but realizing the necessity to include additional correlation for these types of problems. It also stresses the importance of obtaining  $\sigma$  orbitals in a fashion which does not prejudice the  $\pi$  system with regards to charge localization and delocalization, using MCSCF methodologies.

An inherent philosophical weakness in the use of CNDO and INDO in calculations of weakly interacting dimers is that the methods are parameterized for strongly bound molecules only. From experience, it is known that in the weak interaction region, CNDO/S and INDO/S perform with quantitative precision, but this may not be expected in the strong interaction region where the forces are very large. In addition, these schemes use Nishimoto–Mataga [46,47] integrals as is necessary to correctly describe singlet excited states, but these integrals usually underestimate triplet absorption energies. If the singlet and triplet manifolds remain separate, as is usually the case in the spectroscopy of single molecules, then alternate schemes such as Pariser [48] or Ohno–Klopman integrals can be used specifically to describe the triplet states [49]. Unfortunately, for weakly interacting systems, the individual molecule triplet and singlet manifolds become interwoven, and hence such a pragmatic approach cannot be applied. Hence, normalization of CNDO/INDO results through the study of the triplet states of the isolated chromophores is essential. We see that while quantitative applications of these methods require careful consideration of approximations involved, the main qualitative features associated with the intrusion of spin-forbidden processes in monomers into spin-allowed processes in dimers is believed to be adequately described and quite general in nature.

#### Acknowledgement

J.R.R. is indebted to the Australian Research Council for the provision of a research Fellowship.

#### References

- [1] J.N. Murrell and J. Tanaka, *Mol. Phys.*, 7 (1969) 364.
- [2] D.F. Evans, *J. Chem. Soc.*, (1960) 1735.
- [3] R.J.M. Hobbs, *Ph.D. Thesis*, University of Bristol, UK, 1968, p. 246.
- [4] J. Deisenhofer, O. Epp, K. Miki, R. Huber and H. Michel, *J. Mol. Biol.*, 180 (1984) 385.
- [5] J. Deisenhofer, O. Epp, K. Miki, R. Huber and H. Michel, *Nature (London)*, 318 (1985) 618.
- [6] N.S. Hush and I.S. Woolsey, *Mol. Phys.*, 21 (1971) 465.
- [7] L.A. Schechtman and M.E. Kenney, *Proc. Electrochem. Soc.*, 83 (1983) 340, and refs. therein.
- [8] J.R. Reimers and N.S. Hush, *Chem. Phys.*, 146 (1990) 89.

- [9] M.T. Gandolfi, T. Zappi, R. Ballardini, L. Prodi, V. Balzani, J.F. Stoddart, J.P. Mathias and N. Spencer, *Gazz. Chim. Ital.*, *121* (1991) 521.
- [10] R.B. Campbell, J.M. Robertson and J. Trotter, *Acta Crystallogr.*, *15* (1962) 289.
- [11] S. Tsuzuki and K. Tanabe, *J. Phys. Chem.*, *96* (1992) 10804.
- [12] P. Jungwirth and T. Bally, *J. Am. Chem. Soc.*, *115* (1993) 5783.
- [13] M. Braga and S. Larsson, *Int. J. Quantum Chem.*, *44* (1992) 839.
- [14] M.P. Fülischer, K. Andersson and B.O. Roos, *J. Phys. Chem.*, *96* (1992) 9204.
- [15] P.-A. Malmqvist, B.O. Roos, M.P. Fülischer and A.P. Rendell, *Chem. Phys.*, *162* (1992) 359.
- [16] V. Galasso, *Chem. Phys.*, *153* (1991) 13.
- [17] J. Del Bene and H.H. Jaffé, *J. Chem. Phys.*, *48* (1968) 1807, 4050.
- [18] R.L. Ellis, G. Kuehnlenz and H.H. Jaffé, *Theor. Chim. Acta*, *26* (1972) 131.
- [19] J.E. Ridley and M.C. Zerner, *Theor. Chim. Acta*, *32* (1973) 111.
- [20] A.D. Bacon and M.C. Zerner, *Theor. Chim. Acta*, *53* (1979) 21.
- [21] J.R. Reimers and N.S. Hush, *J. Phys. Chem.*, (1994) submitted for publication.
- [22] N.S. Hush, A.T. Wong, G.B. Bacskay and J.R. Reimers, *J. Am. Chem. Soc.*, *112* (1990) 4192.
- [23] J. Paldus and J. Čížek, *J. Chem. Phys.*, *54* (1971) 2293.
- [24] G.B. Bacskay, G. Bryant and N.S. Hush, *Int. J. Quantum Chem.*, *31* (1987) 471.
- [25] A.T. Amos and G.G. Hall, *Proc. Roy. Soc. London, Ser. A*, *263* (1971) 483.
- [26] H.F. King, R.E. Stanton, H. Kim, R.E. Wyatt and R.G. Parr, *J. Chem. Phys.*, *47* (1967) 1936.
- [27] W.D. Edwards and M.C. Zerner, *Theor. Chim. Acta*, *72* (1987) 347.
- [28] R. Pariser and R.G. Parr, *J. Chem. Phys.*, *21* (1953) 466.
- [29] R. Pople, *Trans. Faraday Soc.*, *49* (1953) 1375.
- [30] S. Hu and T.G. Spiro, *J. Am. Chem. Soc.*, *115* (1993) 12029.
- [31] E.T. Shimomura, M.A. Phillippi, H.M. Goff, W.F. Scholz and C.A. Reed, *J. Am. Chem. Soc.*, *103* (1981) 6778.
- [32] N.L. Bauld, *Tetrahedron*, *45* (1989) 5307.
- [33] S. Larsson, *J. Am. Chem. Soc.*, *103* (1981) 4034.
- [34] G. Herzberg, *Molecular Spectra and Structure. III. Electronic Spectra and Electronic Structure of Polyatomic Molecules*, Van Nostrand, Princeton, NJ, 1966.
- [35] J.W. Stocker, S. Hug and S.G. Boxer, *Biochim. Biophys. Acta*, *1144* (1993) 325.
- [36] W.W. Parson, E. Nabedryk and J. Breton, in J. Breton and A. Verméglio (eds.), *The Photosynthetic Reaction Centre II: Structure, Spectroscopy and Dynamics*, NATA, New York, 1992, p. 79.
- [37] J. Breton, E. Nabedryk and W.W. Parson, *Biochemistry*, *31* (1992) 7503.
- [38] G. Corongiu and E. Clementi, *J. Chem. Phys.*, *69* (1978) 4885.
- [39] L. Takiff and S.G. Boxer, *J. Am. Chem. Soc.*, *110* (1988) 4425.
- [40] J.R. Reimers and N.S. Hush, *Inorg. Chem.*, *29* (1990) 3686.
- [41] P. Ford, D.F.P. Rudd, R. Gaunder and H. Taube, *J. Am. Chem. Soc.*, *90* (1968) 1187.
- [42] J. Zeng, N.S. Hush and J.R. Reimers, manuscript in preparation.
- [43] J.P. Doering and J.H. Moore, Jr., *J. Chem. Phys.*, *56* (1972) 2176.
- [44] S. Japar and D.A. Ramsay, *J. Chem. Phys.*, *58* (1973) 5832.
- [45] P.S. Egel and B.M. Monroe, *Adv. Photochem.*, *8* (1970) 302.
- [46] K. Nishimoto and N. Mataga, *Z. Phys. Chem.*, *12* (1957) 335.
- [47] K. Nishimoto and N. Mataga, *Z. Phys. Chem.*, *13* (1957) 140.
- [48] R. Pariser and R.G. Parr, *J. Chem. Phys.*, *21* (1953) 767.
- [49] E. Lindholm and L. Åsbrink, *Molecular Orbitals and their Energies as studied by the Semiempirical HAM Method*, Springer, Berlin, 1985, p. 147.